Spin Dynamic Study on the Electric Field Dependence of Carrier Generation

Fuyuki Ito, Tadaaki Ikoma,* Kimio Akiyama, and Shozo Tero-Kubota

Institute of Multidisciplinary Research for Advanced Materials, Tohoku University, Sendai 980-8577, Japan

Received: December 5, 2004; In Final Form: January 28, 2005

Using an acceptor-doped poly(*N*-vinylcarbazole) film, the magnetic field effect (MFE) on the generation efficiency of photoinduced charge was measured under various electric fields in order to clarify how the applied electric field affects the elementary processes in the photocarrier generation in photoconductive polymeric molecular solids. The external magnetic field influenced the electron spin dynamics among the geminate electron−hole pairs within a scale of a few nanometers and decreased the photocarrier generation efficiency. The observed MFE due to a hyperfine mechanism was almost independent of the electric field. By employing the stochastic Liouville equations based on a one-dimensional lattice model, we performed some model calculations for the dissociation, hopping, and recombination rate dependence of MFE on the generation efficiency. From a comparison between the observed and calculated MFE, it was concluded that the electric field affects the dissociation more than the hopping and the recombination. This coincides with the concepts in the Onsager model that is used to analyze the electric field dependence of carrier generation efficiency so far. The one-dimensional lattice model is a proper model for the carrier generation in polymeric molecular solids, which is qualitatively consistent with the Onsager model except for the long-range hole jump.

Introduction

The generation efficiency of photoinduced carriers in photoconductive molecular solids depends on the external electric field and temperature.[1−3] In general, the source of these dependences of the generation efficiency has been attributed to geminate recombination, where the same electron (e) and hole (h) which have been created by the absorption of a single photon recombine with each other. The Onsager theory (Scheme 1), which originally deals with the separation probability of a thermalized e−h pair in an isotropic medium,[4,5] apparently fits the electric-field-assisted dissociation of charged particles even in molecular solids with low dielectric constants.

Two assumptions are made in the Onsager model for the electric field dependence of the generation efficiency in molecular solids. First, a photon somehow creates an e−h pair and its yield (φ_0) is electric-field-independent. Second, the dissociation probability from the e−h pair (φ_d) is determined by three factors: the attractive Coulomb interaction between e and h, the repulsive electrostatic interaction with the external electric field, and the Brownian motion due to thermal energy. r_t is the initial e−h separation distance where the electrostatic energy is balanced with the total excitation energy including heat. Based on the Onsager model above, the analysis of the electric field dependences of the carrier generation efficiency and the recombination yield suggests the presence of e−h pairs having a fairly large r_t of 2−3 nm.[6−16] This long separation has been usually rationalized by thermalization that is a rapid conversion of excess molecular energy after the light excitation to the kinetic energy of charged molecules. Such an intermolecular energy flow is less likely in a molecular system in which the internal conversion effectively takes place within a single molecule due to strong intramolecular vibronic and spin−orbit couplings. Nevertheless, the Onsager model has been accepted for a long time because of great success in reproducing experimental data very well.

SCHEME 1: Onsager and One-Dimensional Lattice Models for the Carrier Generation Process

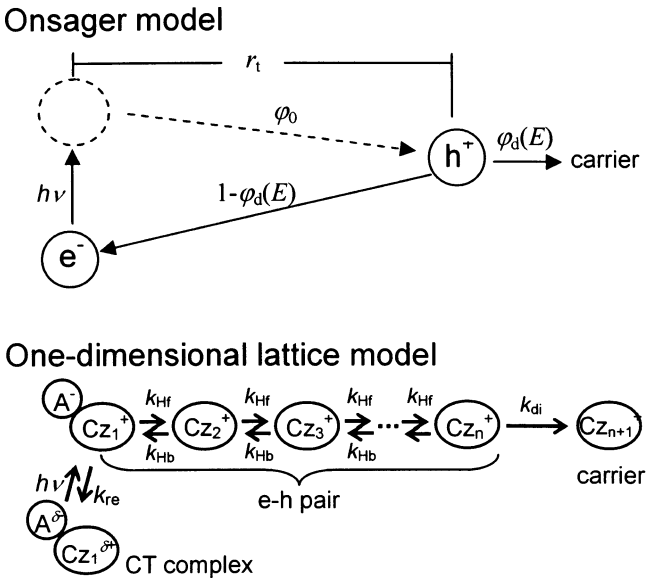

Recent spectroscopic and modern theoretical studies allow us to have more detailed information about the geminate e−h pair dynamics.[17−28] For example, by means of time-resolved electron spin resonance spectroscopy, we succeeded in directly detecting the geminate e−h pairs captured in trap sites in an electron acceptor (A)-doped poly(*N*-vinylcarbazole) (PVCz) film and proving a large population of e−h pairs with a separation

* To whom correspondence should be addressed. Tadaaki Ikoma, IMRAM, Tohoku University, Katahira 2-1-1, Aobaku, Sendai 980-8577, Japan. Telephone: +81-22-217-5614. Fax: +81-22-217-5612. E-mail: ikoma@tagen.tohoku.ac.jp.

10.1021/jp044475e CCC: $30.25
Published on Web 03/19/2005

distance of less than 1 nm.[17,20] In other papers,[18,19] based on magnetic field effects (MFE) on the charge recombination and escape yields in the film sample, we proposed a one-dimensional lattice model for carrier generation as illustrated in Scheme 1. In this model, e and h separate and approach each other by stepwise hole hops between the neighboring carbazole (Cz) units rather than a long-range hole jump by thermalization. The boundary e−h pair at the last pair site corresponds to the distant e−h pair in the Onsager model. The analysis on the one-dimensional lattice model also gives a 2−3 nm separation at the boundary e−h pair. In this way, the MFE experiments enabled us to perform a detailed study on the spin dynamics of the geminate e−h pairs on a nanometer scale. However, the validity of two important assumptions related to the electric-field-independent and -dependent elementary processes in the Onsager model has not been examined yet. Moreover, lately the concern with the electric field dependence of the MFE on the ionic pair dynamics has been growing from the viewpoints of material and biological science.[29−35]

First of all in this paper, we carried out some model calculations for the MFE on the carrier generation efficiency using stochastic Liouville equations (SLE) based on the one-dimensional lattice model. The model calculations using various rate constants clarified how the elementary process influences the MFE on the generation efficiency. Next, the paper describes the electric field dependence of the MFE on the generation efficiency of photoinduced carriers for a 1,2,4,5-tetracyanobenzene (TCNB)-doped PVCz film observed at room temperature. From a comparison between the experimental and calculated results, we examined the relation between the one-dimensional and Onsager models.

Experimental Section

PVCz with a mean unit number of around 5.7×10^3 (Aldrich) was purified before use by reprecipitation with toluene and ethanol. TCNB (Tokyo Kasei) recrystallized from ethanol was employed. The TCNB-doped (3 mol %) PVCz films were cast on a quartz substrate coated with a transparent electrode (indium tin oxide, ITO). To form a sandwich type cell, the surface of the TCNB-doped PVCz film was coated with a semitransparent circular Au electrode of 1.96×10^{-5} m^2 using a vacuum vapor deposition method (ULVAC Kiko, VPC-260). This sandwich cell has the configuration of blocking electrodes for the TCNB-doped PVCz sample. The thicknesses of the ITO electrode, the TCNB-doped PVCz film, and the Au electrode were 62 nm, 3.4 μm, and 160 nm, respectively. The light to excite the sample was irradiated from the side of the quartz glass as shown in Figure 1.

To apply the magnetic field, the film samples fixed by a holder made of nonmagnetic materials were placed between the pole pieces of an electromagnet. The magnetic field strength was controlled by two variable power supplies (Takasago, GP060-30R and GP050-2) and measured with a Hall-type gaussmeter (F. W. BEL, 4048). The second harmonic wave (532 nm, 2.33 eV) of a nanosecond Nd^{3+}:YAG laser (Spectra-Physics, INDI-40-20), which had a full width at half-maximum of 23 ns, was utilized as the excitation light. The intensity and size of the laser beam were controlled by ND filters and a pinhole placed before the sample in order to properly illuminate the samples. The transient phenomena of the photoinduced charge were measured with an *RC* series circuit which comprised the sample cell with a capacitance (*C*) of 147 pF, a resistance (*R*) of 0.9 MΩ, and a bipolar DC power supply (Matsusada Precision, PLE-160-0.45).[11,19] The *C* and *R* of the sample cell

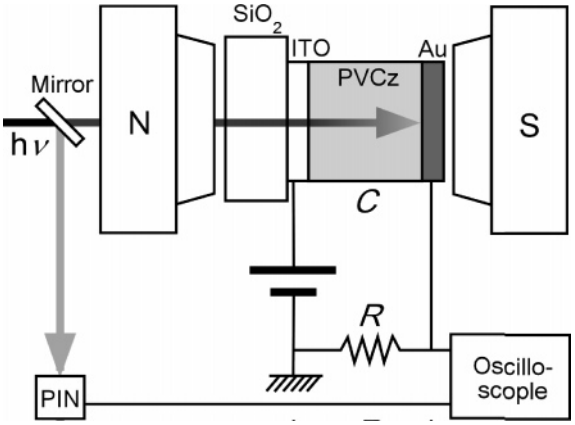

Figure 1. Schematic diagram of an experimental setup for the measurements of the magnetic and electric field dependences of the photoinduced charge.

were measured by an LCR meter (Hioki, 3532-50). The electric potential at the Au electrode ($\Delta V(t)$) was monitored as a function of the delay time after the laser flash by a 500 MHz digital oscilloscope (Tektronix, TDS-520D). In the circuit with the large *R*, the change in surface potential is equal to a value proportional to the difference in net charge ($Q(t)$) on the Au electrode: $\Delta V(t) = Q(t)/C$. The intensity fluctuation of the photoinduced charge resulting from the power stagger of the excitation light was corrected by monitoring every laser flash using a PIN diode (Hamamatsu, C1083). All measurements were performed at room temperature.

Theoretical Calculations

As illustrated in Scheme 1, the elementary processes in the one-dimensional lattice model for the carrier generation can be classified into three groups: dissociation (k_{dis}), hopping (k_{H_f} and k_{H_b}), and recombination (k_{re}). k_{dis} is a rate constant for the final process to escape from the boundary e−h pair to the free carrier. k_{H_f} and k_{H_b} are the mean rate constants for the forward and backward hole hops among the geminate e−h pairs, respectively. k_{re} is a rate constant for the annihilation of e and h, which occurs only from a singlet spin state of the contact e−h pair. A reasonable correspondence between the processes of the Onsager and one-dimensional lattice models can be found because of their similarity. It can be said that the dissociation from the distant e−h pair in the Onsager model is the k_{dis} process. The effective time of the distant e−h pair in the Onsager model is governed by the kinetic balance between the k_{H_f} and k_{H_b} processes. The k_{re} process is closely related to the recombination probability in the Onsager model.

On the supposition that the electric field may affect the elementary processes, it is valuable to simulate how the kinetic rate constants influence the MFE on the carrier generation efficiency. The theoretical calculation with the SLE is useful for simulation of radical pair dynamics. The SLE taking into account eight geminate e−h pairs can be written as follows.

$$\begin{cases} \dot{\rho}_0(t) = k_{re}\rho_1(t)_{SS} \\ \dot{\rho}_1(t) = -i[\hat{H}_1,\rho_1(t)] - k_{H_f}\rho_1(t) + k_{H_b}\rho_2(t) - k_{re}\rho_1(t)_{SS} \\ \dot{\rho}_2(t) = -i[\hat{H}_2,\rho_2(t)] + k_{H_f}\rho_1(t) - (k_{H_f} + k_{H_b})\rho_2(t) + k_{H_b}\rho_3(t) \\ \vdots \\ \dot{\rho}_8(t) = -i[\hat{H}_8,\rho_8(t)] + k_{H_f}\rho_7(t) - (k_{H_b} + k_{dis})\rho_8(t) \end{cases} \quad (1)$$

ρ_0 and ρ_n are the density operators for a recombined molecule in the ground singlet state and of the *n*th e−h pair (cf. Scheme

SCHEME 2: MFE of the Hyperfine Mechanism Due to Distant e−h Pairs

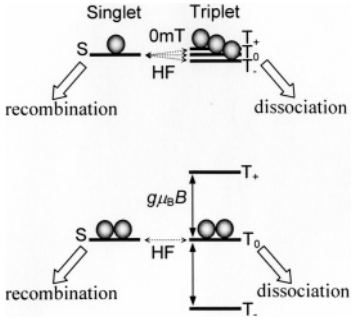

1). $\hat{H}_n$ is a spin Hamiltonian for the nth e−h pair written by

$$\hat{H}_n = -J_n\left(\frac{1}{2} + 2\hat{S}_1\hat{S}_2\right) + \sum_{i,j} A_{i,j}\hat{\mathbf{S}}_i\hat{\mathbf{I}}_{i,j} + \sum_i g_i\mu_B B\hat{S}_{iz} \quad (2)$$

$\mathbf{S}_i$ and $\mathbf{I}_{i,j}$ denote the electron operator of the ith component molecule ($i = 1,2$) and the nuclear spin operator of the jth nucleus in the ith component molecule, respectively. J is the exchange interaction constant and $A_{i,j}$ is the hyperfine coupling constant of the jth nucleus in the ith component. g, μ_B, and B stand for the g-factor, the Bohr magneton, and the applied magnetic field, respectively. All the magnetic parameters for the TCNB-doped PVCz film system such as J_n, A_{ij}, and g_i have already been determined in the previous paper.[19] The MFE on the gross carrier generation efficiency (φ) is defined by the ratio between the efficiency difference induced by applying a magnetic field and the efficiency in the absence of the magnetic field.

$$\mathrm{MFE}(B) = \frac{\varphi(B) - \varphi(0)}{\varphi(0)} \quad (3)$$

where $\varphi = 1 - \rho_0(\infty)$. Because the hole spin dynamics begins from the contact e−h pair, the initial condition of the SLE is set on $\rho_1(0)_{SS} = 1$. We obtained the MFE at B =10 mT by numerically solving the SLE of eq 1. The MFE at 10 mT is dominated by the hyperfine mechanism (HFM), which originates from the Zeeman interaction in the e−h pairs having the exchange interaction smaller than the hyperfine interaction as shown in Scheme 2.[19,36]

At zero magnetic field, four spin states of the e−h pair without significant exchange interaction are degenerate in energy. Hence the hyperfine interaction can give rise to the population transfer between the singlet and triplet states. Under a magnetic field, on the other hand, the hyperfine interactions between the singlet state and two of the triplet states (T_+ and T_-) are not efficient because the triplet states are split into three levels by the Zeeman interaction. In the case of e−h pairs born from a singlet state, the reduction of effective hyperfine interaction results in the increase of the singlet population and the decrease of the triplet population. In the TCNB-doped PVCz film, the recombination occurs only from the singlet pair and thus the triplet pair must dissociate. The population change induced by the Zeeman interaction in e−h pairs with negligible J constants, which correspond to the 3-8th pairs in the one-dimensional lattice model, is a cause of HFM-MFE on the carrier generation efficiency. Hence the effective time for the long distant e−h pairs to interact with the applied external magnetic field is important.

Figure 2a shows the dissociation rate dependence of the MFE using a kinetic parameter set of $k_{H_f} = k_{H_b} = 4.5 \times 10^8\ s^{-1}$ and

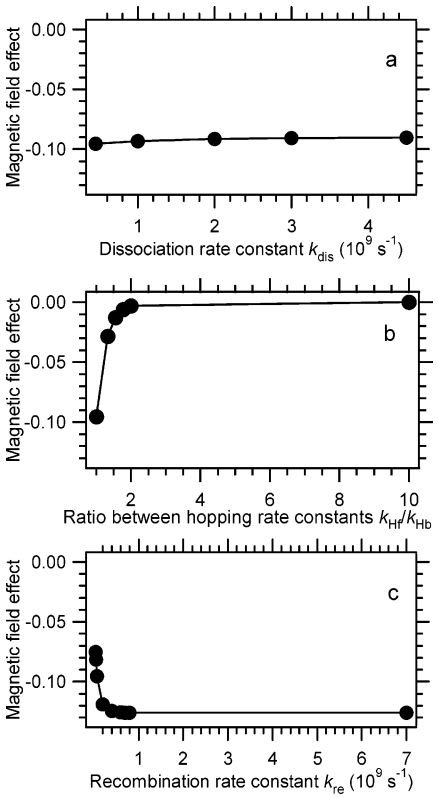

Figure 2. Dissociation (a), hopping (b), and recombination (c) rate dependences of the HFM-MFE on the carrier generation efficiency at 10 mT calculated by the SLE for the one-dimensional lattice model consisting of eight e−h pairs.

$k_{re} = 7.0 \times 10^7\ s^{-1}$. The external electric field might accelerate the dissociation rate. The calculated MFE remains constant even though k_{dis} varies from 4.5×10^8 to $4.5 \times 10^9\ s^{-1}$. This is because the change in k_{dis} has a minor effect on the total mean lifetime of the long distant e−h pairs. The increase in the dissociation rate shortens the length of the hole's stay at only the 8th boundary e−h pair but leaves the hole kinetics at the rest of the pairs. Even in the case of fast dissociation, consequently, the gross period for the long distant e−h pairs is long enough to induce a constant HFM-MFE.

Next, we examined the hopping rate dependence of the HFM-MFE. The variation in the hopping rate should exert a serious effect because of the stepwise connections among all e−h pairs. It might be considered that the electric field increases the forward hopping rate more than the backward one. Figure 2b shows the relative hopping rate dependence of the MFE using kinetic parameters of $k_{dis} = 4.5 \times 10^8\ s^{-1}$ and $k_{re} = 7.0 \times 10^7\ s^{-1}$. The calculated MFE dramatically diminishes with an increase in the k_{H_f}/k_{H_b} ratio. The decrease in MFE is attributed to a deviation of the kinetic balance in stepwise hopping, which indicates a one-way dissociative reaction. For example, the φ becomes almost 1 for $k_{H_f}/k_{H_b} = 10$, where the recombination hardly takes place. In the case of the e−h pair dynamics without the spin selective recombination (cf. Scheme 2), the MFE does not appear, even though the lifetime of the distant e−h pair is long.

On the other hand, it should be noted that the MFE increases in the case of almost a one-side dynamics toward the recombination. Figure 2c shows the recombination rate dependence of the HFM-MFE. In this calculation, we adopted a parameter set of $k_{H_f} = k_{H_b} = k_{dis} = 4.5 \times 10^8\ s^{-1}$. As the recombination rate increases, the MFE of carrier generation efficiency becomes larger and saturates at a level. The increase of MFE can be

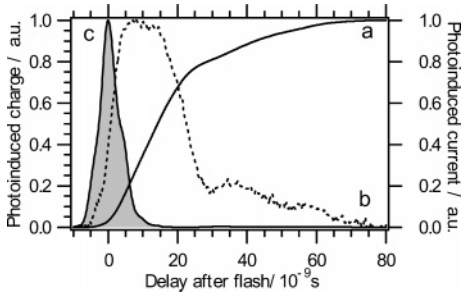

Figure 3. (a) Time profile of the charge induced by pulse light irradiation at $\lambda = 532$ nm under an electric field of 3.5×10^5 V/cm. (b) Transient photocurrent obtained by numerical differentiation of the observed time profile of curve a. (c) Excitation profile of the pulse laser.

interpreted in terms of a necessary condition for the appearance of MFE, which is the spin selective recombination. However, too fast recombination is unfavorable in the HFM-MFE because the e−h pair needs to undergo the distant pairs. Probably these contrary effects would operate behind the saturation of the calculated MFE level in the range of large k_{re}. The change of k_{re} could be caused by applying the electric field. If the contact e−h pair state with respect to the ground state is located in an inverted region within the framework of the Marcus theory,[28] the stabilization of the state energy of the e−h pair due to the external electric field may lead to an increase in k_{re}. After all, the model calculations using SLE clarified that the three kinds of rate constant dependences of MFE are quite different from each other.

Results and Discussion

In the visible light region, the TCNB-doped PVCz has a broad absorption band due to the charge-transfer (CT) complex between TCNB and the neighboring Cz's. The irradiation of the doped sample at a wavelength (λ) of 532 nm corresponds to a selective excitation of the CT complex among the randomly oriented Cz chromophores. Figure 3a shows the time profile of the photoinduced charge measured by the selective CT excitation at room temperature. Even when the polarity of the electrode was changed, the amplitude of the signal remained, although the signal phase was inverted. Based on hole conductivity of the PVCz amorphous film, the observation of equal intensity of the forward and backward signals indicates a uniform photoexcitation of the CT complex along the direction of the film thickness. In the observed time profile of the photocharge, a fast rise up to 30 ns after the laser pulse and a slow rise after 30 ns appeared. Figure 3b depicts the time profile of photoinduced current in the TCNB-doped PVCz film, which was obtained by numerical differentiation of the observed photocharge profile. The fast decay up to 30 ns and a slow decay after 30 ns of the calculated photocurrent originate from the charge recombination of the geminate and the free e−h pairs, respectively.[19] Therefore, the observed photocharge at 30 ns can be taken as the total charge that could escape from the geminate recombination process.

Figure 4a shows the electric field dependence of the time profile of photoinduced charge in the absence of a magnetic field. The photocharge decreases in intensity with the decrease in the electric field, but the fast rise due to the escape from the geminate pair and the slow rise due to the drift of free ions clearly appeared in any electric field. The carrier generation efficiency (φ) for a particular electric field E, which is equivalent

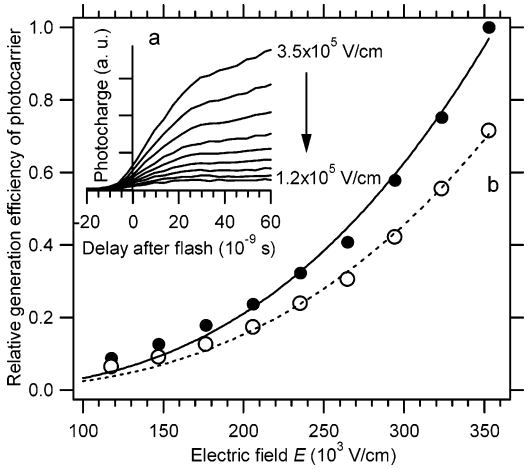

Figure 4. (a) Electric field dependence of the photoinduced charge profile observed in the absence of a magnetic field. (b) Electric field dependence of the escaped charge observed at 0 mT (closed circles) and 10 mT (open circles). The solid and broken lines indicate the functions of $\varphi = \alpha E^m$ fitting the experimental data at 0 and 10 mT, respectively.

to the escape yield of a hole, is derived from the photocharge (Q_{esc}).

$$\varphi(E) = \frac{Q_{esc}(E)}{eF} \tag{4}$$

where e and F are the electronic charge and the absorbed photon number in the film, respectively.[6] Although the F value could not be estimated experimentally, the photocharge at 30 ns can be regarded as the relative carrier generation efficiency according to the proportionality between φ and Q_{esc}. In Figure 4b, the observed photocharge at 30 ns is plotted against the applied electric field. It is clearly seen that the φ value nonlinearly varies with the electric field. In the electric field region of a few 10^5 V/cm, the generation efficiency is approximated by a power law of[6]

$$\varphi(E) = \varphi_0 Y_0 E^m = \alpha E^m \tag{5}$$

Y_0 is a constant for proportionality. As shown by the solid line in Figure 4b, in fact the observed electric field dependence of the carrier generation efficiency was well fitted by a power function with the parameters of $\alpha = 1.19 \times 10^{-15}$ and $m = 2.69$. The optimized power of $m = 2.69$ is reduced to a distance of $r_0 = 1.8-2.0$ nm of the distant e−h pair in the Onsager model.[6]

In the presence of a magnetic field, on the other hand, similar time profiles of the photocharge with the fast and slow rises were observed. From the fast component due to escape from the geminate recombination, we obtained the electric field dependence of φ in the presence of the magnetic field as shown by the open circles in Figure 4b. The electric field dependence at 10 mT also indicated a nonlinear relationship, but in all electric fields, the generation efficiency was smaller than that at 0 mT. A power function with $\alpha = 8.66 \times 10^{-16}$ and $m = 2.69$ well reproduced the experimental data. The same m values in the optimized fitting functions for 0 and 10 mT suggest that the magnetic field does not alter which e−h pair serves as the thermalized pair in the Onsager model, from which the electric-field-assisted carrier generation occurs. However, the reduction of φ by applying a magnetic field of 10 mT indicates the MFE on the dynamics of e−h pairs. The MFE is calculated to be

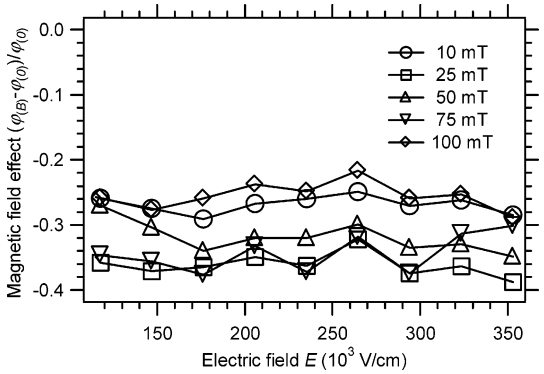

Figure 5. Electric field dependence of MFE on the carrier generation efficiency observed in several magnetic fields.

−0.27 from the difference in the α values. The negative MFE at 10 mT is basically interpreted in terms of the HFM in the distant e−h pairs born from the singlet state.[19] The definition of $[\alpha(10\text{mT}) - \alpha(0\text{mT})]/\alpha(0\text{mT})$ for MFE is reduced to $[\varphi_0(10\text{mT}) - \varphi_0(0\text{mT})]/\varphi_0(0\text{mT})$. Hence the observation of MFE on the α parameter indicates that the generation efficiency of the distant e−h pair in the Onsager model is independent of the electric field but it depends on the magnetic field.

Figure 5 represents the electric field dependence of MFE on the photocarrier generation efficiency measured in various magnetic fields. The observed MFE shows a negative effect of ca. −0.31, meaning a 31% decrease in the generation efficiency due to the magnetic fields. This constant decrease due to magnetic fields larger than the hyperfine interactions of the component molecules arises from the HFM-MFE on the singlet born e−h pairs. Moreover, it should be noted that the MFE does not change very much with the electric field. Such constant behavior of the MFE relative to the electric field is similar to the calculated k_{dis}-dependence of MFE, and it is different from the k_{H_f}/k_{H_b}- and k_{re}-dependencies. Thus, these facts indicate that the electric field affects the dissociation process rather than the hopping and recombination processes. This conclusion does not contradict the Onsager model, in which the generation process of the distant e−h pair is independent of the external electric field, although the dissociation probability from the distant e−h pair depends on the electric field.

The applied electric field of less than 10^6 eV/cm is comparable to the mutual Coulomb interaction of the long distant e−h pair with a separation distance of a few nanometers. Such electric fields may be a negligible level within the separation distances below a few nanometers. This is the main reason why only the dissociation kinetics from the long distant e−h pair is effectively influenced under the electric fields and the Onsager theory can apparently fit the electric field effect (EFE) on carrier generation yield. On the other hand, an applied magnetic field of less than 100 mT is large enough to perturb the spin dynamics of the middle distant e−h pairs, because the magnetic interactions even in the e−h pairs at less than 2 nm are not very large. Therefore, it can be said that the MFE experiments clarified the separation and recombination dynamics in the short distances that were not accessible in the past EFE experiments. Regarding the combination of the MFE and EFE experiments, it is concluded that the one-dimensional lattice is a proper model for the carrier generation process, although the Onsager model expresses well the electric field independency of the boundary e−h pair generation and the electric-field-assisted dissociation from that pair.

Conclusion

In summary, we have investigated the carrier generation by the electric field dependence of the MFE on the carrier generation efficiency. The generation efficiency increased with an increase in the external electric field, but the MFE on the generation efficiency did not depend on the electric field. From a comparison with the model calculations based on the SLE analysis, it was concluded that the electric field affects the last dissociative step from the boundary distant e−h pair and has a negligible effect on the stepwise hole hops in the generation process of the distant e−h pair. Although these facts support the validity of the concepts in the Onsager model, the one-dimensional lattice model is a proper model that can explain not only the EFE but also the MFE experimental results.

Acknowledgment. T.I. thanks Mr. T. Ogiwara (Tohoku University) for his assistance in the experiments. This study was financially supported by Grant-in-Aid for Scientific Research No. 15310069 from the Ministry of Education, Culture, Sports, Science, and Technology (MEXT) of the Japanese Government, the Murata Science Foundation.

References and Notes

(1) Pearson, J. M.; Stolka, M. *Poly(N-vinylcarbazole)*; Gordon and Breach: New York, 1981.

(2) Mort, J.; Pai, D. M. *Photoconductivity and Related Phenomena*; Elsevier: Amsterdam, 1976; Chapters 7, 8, 10, and 11.

(3) Mort, J.; Pfister, G. In *Electronic Properties of Polymers*; Mort, J., Pfister, G., Eds.; Wiley-Interscience: New York, 1982; Chapter 6.

(4) Onsager, L. *J. Chem. Phys.* **1934**, *2*, 599.

(5) Onsager, L. *J. Chem. Phys.* **1938**, *54*, 554.

(6) Melz, P. J. *J. Chem. Phys.* **1972**, *57*, 1694.

(7) Okamoto, K.; Itaya, A. *Bull. Chem. Soc. Jpn.* **1984**, *57*, 1626.

(8) Yokoyama, M.; Endo, Y.; Mikawa, H. *Bull. Chem. Soc. Jpn.* **1976**, *49*, 1538.

(9) Yokoyama, M.; Endo, Y.; Matsubara, A.; Mikawa, H. *J. Chem. Phys.* **1981**, *7*, 30065.

(10) Yokoyama, M.; Shimokihara, S.; Matsubara, A.; Mikawa, H. *J. Chem. Phys.* **1982**, *76*, 724.

(11) Borsenberger, P. M.; Ateya, A. I. *J. Appl. Phys.* **1978**, *49*, 4035.

(12) Borsenberger, P. M.; Contois, L. E.; Hoesterey, D. C. *J. Chem. Phys.* **1978**, *68*, 637.

(13) Pfister, G.; Williams, D. J. *J. Chem. Phys.* **1974**, *61*, 2416.

(14) Borsenberger, P. M.; Chowdry, A.; Hoesterey, D. C.; Mey, W. *J. Appl. Phys.* **1978**, *49*, 5555.

(15) Wang, Y. *Nature* **1992**, *356*, 585.

(16) Wang, Y.; West, R.; Yuan, C. *J. Am. Chem. Soc.* **1993**, *115*, 3844.

(17) Ikoma, T.; Nakai, M.; Akiyama, K.; Tero-Kubota, S. *Angew. Chem., Int. Ed.* **2001**, *40*, 3234.

(18) Ito, F.; Ikoma, T.; Akiyama, K.; Kobori, Y.; Tero-Kubota, S. *J. Am. Chem. Soc.* **2003**, *125*, 4722.

(19) Ito, F.; Ikoma, T.; Akiyama, K.; Tero-Kubota, S.; Watanabe, A. *J. Phys. Chem. B*, in press.

(20) Ikoma, T.; Akiyama, K.; Tero-Kubota, S. *Phys. Rev. B*, in press.

(21) Miyasaka, H.; Moriyama, T.; Kotani, S.; Muneyasu, R.; Itaya, A. *Chem. Phys. Lett.* **1994**, *225*, 315.

(22) Miyasaka, H.; Moriyama, T.; Ide, T.; Itaya, A. *Chem. Phys. Lett.* **1998**, *292*, 339.

(23) Abramavicius, D.; Gulbinas, V.; Ruseckas, A.; Undzenas, A.; Valkunas, L. *J. Chem. Phys.* **1999**, *111*, 5611.

(24) Abramavicius, D.; Gulbinas, V.; Valkunas, L. *Synth. Met.* **2000**, *109*, 39.

(25) Noolandi, J.; Hong, K. M. *J. Chem. Phys.* **1979**, *70*, 3230.

(26) Kalinowski, J.; Stampor, W.; Di Marco, P. G. *J. Chem. Phys.* **1992**, *96*, 4136.

(27) Braun, C. L. *J. Chem. Phys.* **1984**, *80*, 4157.

(28) Wang, Y.; Suna, A. *J. Phys. Chem. B* **1997**, *101*, 5627.

(29) Ohta, N.; Koizumi, M.; Umeuchi, S.; Nishimura, Y.; Yamazaki, I. *J. Phys. Chem.* **1996**, *100*, 16466.

(30) Ohta, N. *Bull. Chem. Soc. Jpn.* **2002**, *75*, 1637.

(31) Mizoguchi, M.; Ohta, N. *Chem. Phys. Lett.* **2003**, *372*, 66.
(32) Kalinowski, J.; Cocchi, M.; Virgili, D.; Marco, P. D.; Fattori, V. *Chem. Phys. Lett.* **2003**, *380*, 710.
(33) Kalinowski, J.; Szmytkowski, J.; Stampor, W. *Chem. Phys. Lett.* **2003**, *378*, 380.
(34) Horiuchi, M.; Maeda, K.; Arai, T. *Appl. Magn. Reson.* **2003**, *23*, 309.
(35) Miura, T.; Maeda, K.; Arai, T. *J. Phys. Chem. B* **2003**, *107*, 6474.
(36) Hayashi, H. In *Dynamic Spin Chemistry*; Nagakura, S., Hayashi, H., Azumi, T., Eds.; Kodansha: Tokyo, 1998; Chapter 2.